

# Gray and White Matter Asymmetries in Healthy Individuals Aged 21–29 Years: A Voxel-Based Morphometry and Diffusion Tensor Imaging Study

Hidemasa Takao,<sup>1\*</sup> Osamu Abe,<sup>1</sup> Hidenori Yamasue,<sup>2</sup> Shigeki Aoki,<sup>3</sup>  
Hiroki Sasaki,<sup>1</sup> Kiyoto Kasai,<sup>2</sup> Naoki Yoshioka,<sup>1</sup> and Kuni Ohtomo<sup>1</sup>

<sup>1</sup>Department of Radiology, Graduate School of Medicine, University of Tokyo,  
7-3-1 Hongo, Bunkyo-ku, Tokyo, Japan

<sup>2</sup>Department of Neuropsychiatry, Graduate School of Medicine, University of Tokyo,  
7-3-1 Hongo, Bunkyo-ku, Tokyo, Japan

<sup>3</sup>Department of Radiology, Juntendo University School of Medicine, 3-1-3 Hongo,  
Bunkyo-ku, Tokyo, Japan

---

**Abstract:** The hemispheres of the human brain are functionally and structurally asymmetric. The study of structural asymmetries provides important clues to the neuroanatomical basis of lateralized brain functions. Previous studies have demonstrated age-related changes in morphology and diffusion properties of brain tissue. In this study, we simultaneously explored gray and white matter asymmetry using voxel-based morphometry (VBM) and diffusion tensor imaging (DTI) in 109 young healthy individuals (58 females and 51 males). To eliminate the potential confounding effects of aging and handedness, we restricted the study to right-handed subjects aged 21–29 years. VBM and voxel-based analysis of fractional anisotropy (FA) maps derived from DTI revealed a number of gray matter volume asymmetries (including the right frontal and left occipital petalias and leftward asymmetry of the planum temporale) and white matter FA asymmetries (including leftward asymmetry of the arcuate fasciculus, *cingulum*, and corticospinal tract). There was no significant effect of sex on gray and white matter asymmetry. Leftward volume asymmetry of the planum temporale and leftward FA asymmetry of the arcuate fasciculus were simultaneously demonstrated. Post hoc analysis showed that the gray matter volume of the planum temporale and FA of the arcuate fasciculus were positively related (Pearson correlation coefficient, 0.43;  $P < 0.0001$ ). The results of our study demonstrate gray and white matter asymmetry in right-handed healthy young adults and suggest that leftward volume asymmetry of the planum temporale and leftward FA asymmetry of the arcuate fasciculus may be related. *Hum Brain Mapp* 32:1762–1773, 2011. © 2010 Wiley-Liss, Inc.

**Key words:** arcuate fasciculus; brain; fractional anisotropy; gray matter; lateralization; planum temporale; volume

---

## INTRODUCTION

The hemispheres of the human brain are functionally and structurally asymmetric. The most consistent structural asymmetries are the right frontal and left occipital petalias [Chiu and Damasio, 1980; LeMay, 1977; Toga and Thompson, 2003] and leftward asymmetry of the planum temporale [Geschwind and Levitsky, 1968; Toga and Thompson, 2003]. The right frontal and left occipital

---

\*Correspondence to: Hidemasa Takao, Department of Radiology, Graduate School of Medicine, University of Tokyo, 7-3-1 Hongo, Bunkyo-ku, Tokyo 113-8655, Japan. E-mail: takaoh-tky@umin.ac.jp  
Received for publication 5 November 2009; Revised 15 May 2010; Accepted 12 July 2010  
DOI: 10.1002/hbm.21145  
Published online 30 September 2010 in Wiley Online Library (wileyonlinelibrary.com).

petalias are extensions of the frontal lobe in the right hemisphere and the occipital lobe in the left hemisphere (“petalias” originally referred to the indentations that these extensions make on the inside of the skull). The planum temporale is a triangular-shaped region that occupies the superior temporal plane posterior to the transverse temporal (Heschl’s) gyri, which is engaged in complex auditory processing [Griffiths and Warren, 2002]. It is part of the classical Wernicke’s area, which is responsible for language comprehension. Language is usually lateralized to the left hemisphere of the brain. The study of structural asymmetries provides important clues to the neuroanatomical basis of lateralized brain functions. Evaluating cerebral asymmetry in patients with neurological diseases is also potentially helpful in understanding the etiology of the disease and its symptoms. For example, a number of magnetic resonance (MR) imaging studies have demonstrated reduced or reversed volume asymmetry of the planum temporale in patients with schizophrenia [Hirayasu et al., 2000; Kawasaki et al., 2008; Kwon et al., 1999; Takahashi et al., 2006], which may reflect abnormalities in auditory perception and language processing in patients with schizophrenia.

Language is the most notable and strongly lateralized function in the human brain. Leftward asymmetry of the planum temporale, an extension of Wernicke’s posterior language area, is one of the most consistent structural asymmetries, as mentioned earlier. Some studies have demonstrated leftward asymmetry of the arcuate fasciculus [Büchel et al., 2004; Nucifora et al., 2005; Rodrigo et al., 2007]. The arcuate fasciculus is the tract that connects the frontal and parieto-temporal language areas, classically known as Broca’s and Wernicke’s area, respectively. Although leftward asymmetry of the planum temporale and leftward asymmetry of the arcuate fasciculus were separately reported, the relationship between these two asymmetries is unclear.

The recent development of methods for the analysis of high-resolution MR images of the brain has enabled group differences in brain structure to be investigated on a voxel-by-voxel basis. This methodology, known as voxel-based morphometry (VBM), provides objective and bias-free information about brain structure [Ashburner and Friston, 2000, 2005], which has been increasingly adopted, because manual methods of brain structure measurement can be time consuming, require considerable anatomical expertise, and are limited to brain regions with constant anatomical boundaries. VBM has been applied to investigate cerebral asymmetry in normal individuals and in patients with various diseases [Dorsaint-Pierre et al., 2006; Good et al., 2001a; Hervé et al., 2006; Huster et al., 2007; Kawasaki et al., 2008; Mühlau et al., 2007; Prinster et al., 2006; Shibata, 2007; Watkins et al., 2001]. Some studies have validated this method with structural region of interest (ROI) analyses [Eckert et al., 2008; Luders et al., 2004]. There are several inconsistencies in studies investigating cerebral asymmetry in normal individuals [Good et al., 2001a; Watkins et al., 2001], which may stem from heterogeneity of the populations (e.g., age distribution) from

which study samples are drawn and by the differences in methods of acquisition and measurement of the MR images. A number of studies have demonstrated age-related changes in brain morphology [Abe et al., 2008; Good et al., 2001b; Taki et al., 2004].

In contrast to structural MR imaging, diffusion tensor imaging (DTI) provides subtle information about white matter tissue composition. In biological systems, the diffusion of water is impeded by tissue structures, such as cell membranes, myelin sheaths, intracellular microtubules, and associated proteins. The term “diffusion anisotropy” describes the fact that diffusion occurs most freely in a direction parallel, rather than perpendicular, to an axon or myelin sheath [Moseley et al., 1990]. Measuring anisotropy using DTI is a promising method for noninvasively detecting subtle white matter changes, even if the brain tissue appears normal on conventional MR images [Rovaris et al., 2002; Werring et al., 2000]. Fractional anisotropy (FA) is the most widely used diffusion parameter. Some studies have explored white matter asymmetry using a voxel-based analysis of diffusion tensor (FA) images in normal individuals and/or in patients with schizophrenia [Ardekani et al., 2007; Büchel et al., 2004; Park et al., 2004]. These studies included a relatively small number of subjects with a wide age range. Previous studies have demonstrated age-related alterations in diffusion properties of brain tissue [Abe et al., 2008; Càmarà et al., 2007; Hsu et al., 2008].

In this study, we used VBM to explore gray matter asymmetry in young healthy individuals. To eliminate the potential confounding effects of aging and handedness, we restricted the study to right-handed subjects aged 21–29 years. In addition, we investigated white matter asymmetry using a voxel-based analysis of FA maps derived from DTI. Furthermore, we evaluated the potential relationship between gray and white matter asymmetry. To our knowledge, this is the first study combining VBM and DTI to assess gray and white matter asymmetry.

## MATERIALS AND METHODS

### Subjects

A total of 109 right-handed normal volunteers aged 21–29 years (58 females, mean age =  $26.0 \pm 1.9$  years; 51 males, mean age =  $26.5 \pm 2.4$  years) were included in this study. All subjects were Japanese. Handedness was assessed based on the Edinburgh Inventory [Oldfield, 1971]. All subjects were interviewed by a trained psychiatrist to be screened for the presence or absence of neuropsychiatric disorders through the Structured Clinical Interview for DSM-IV Axis I Disorder, Non-patient Edition (SCID-NP) [First et al., 1997]. These interviews were performed on the same day as the MR scanning. None of the subjects had a history of neuropsychiatric disorder including serious head trauma with known cognitive consequences or loss of consciousness for more than 5 min, psychiatric disorders, or alcohol/substance abuse or dependence. The ethical

committee of the University of Tokyo Hospital approved this study. After a complete explanation of the study to each subject, written informed consent was obtained.

### Imaging Data Acquisition

MR data were obtained on a 1.5-T Signa scanner (GE Medical Systems, Milwaukee, WI). A circularly polarized head coil was used for both radiofrequency pulse transmission and reception of the MR signal. T1-weighted images were acquired using three-dimensional spoiled-gradient recalled acquisition in the steady state (3D-SPGR) in 124 axial slices (repetition time = 40 ms; echo time = 7 ms; flip angle = 30°; field of view = 240 mm; slice thickness = 1.5 mm with no gap; acquisition matrix = 256 × 256; number of excitations = 1) for VBM analysis. The voxel dimensions were 0.9375 mm × 0.9375 mm × 1.5 mm. A single-shot spin-echo echo-planar sequence (repetition time = 6,000 ms; echo time = 78.2 ms;  $b = 1,000$  s/mm<sup>2</sup>; field of view = 240 mm; slice thickness = 5 mm with no gap; acquisition matrix = 128 × 128; number of excitations = 4) was used for diffusion tensor analysis. The acquired volume covered the whole brain and consisted of 30–34 axial slices (in-plane resolution = 1.875 mm × 1.875 mm). Diffusion gradients were always applied on two axes simultaneously around the 180° pulse. Diffusion properties were measured along six noncollinear directions: ( $G_x, G_y, G_z$ ) = [(0, 0, 0), (1/√2, 0, 1/√2), (-1/√2, 0, 1/√2), (0, 1/√2, 1/√2), (0, 1/√2, -1/√2), (1/√2, 1/√2, 0), and (-1/√2, 1/√2, 0)]. Axial proton density and T2-weighted fast spin-echo images were obtained to enable the exclusion of structural abnormalities (repetition time = 3,000 ms; echo time = 28, 84 ms; echo train length = 8; field of view = 240 mm; slice thickness = 3 mm with no gap; acquisition matrix = 256 × 256; number of excitations = 1). A trained radiologist reviewed all scans and found no gross abnormalities such as infarct, hemorrhage, or brain tumors in any of the subjects.

### Diffusion Tensor Map Calculation

The structural distortion of diffusion-weighted images induced by the large diffusion gradients was corrected, based on the corresponding T2-weighted echo-planar images ( $b = 0$  s/mm<sup>2</sup>) [Haselgrove and Moore, 1996; Mangin et al., 2002], using the workstation supplied by the manufacturer (Advantage Workstation, GE Medical Systems). The six independent elements of the 3 × 3 diffusion tensor were calculated for each pixel by using multivariate linear fitting method, according to the Stejskal and Tanner equation:  $S = S_0 \times e^{-bD}$ , where  $S$  is the measured diffusion-weighted signal,  $S_0$  is the signal measured without motion-probing gradients, and  $b$  is the strength of the diffusion-weighting. After diagonalization, three eigenvalues ( $\lambda_1, \lambda_2$ , and  $\lambda_3$ ) and three eigenvectors were obtained. The eigenvalues determine the shape and size of the diffusion

ellipsoid. The FA maps were generated on a voxel-by-voxel basis as follows [Basser et al., 1994]:  $FA = \sqrt{3}/\sqrt{2} \times \sqrt{[(\lambda_1 - MD)^2 + (\lambda_2 - MD)^2 + (\lambda_3 - MD)^2]}/\sqrt{(\lambda_1^2 + \lambda_2^2 + \lambda_3^2)}$ , where MD (mean diffusivity) =  $(\lambda_1 + \lambda_2 + \lambda_3)/3$ .

### Image Processing

Image analysis was performed using statistical parametric mapping (SPM) 5 software (<http://www.fil.ion.ucl.ac.uk/spm>) developed in the Wellcome Department of Imaging Neuroscience, Institute of Neurology, University College London, running in MATLAB 7.5.0 (Mathworks, Sherborn, MA). All image processing steps described below are summarized in Figure 1.

### VBM Asymmetry Processing

The 3D-SPGR images were spatially normalized, bias field corrected, and segmented using an integrated generative model (unified segmentation [Ashburner and Friston, 2005]). Unified segmentation involves alternating between segmentation, bias field correction, and normalization to obtain local optimal solutions for each process. The International Consortium for Brain Mapping (ICBM) gray matter, white matter, and cerebrospinal fluid templates were used as priors to segment and normalize (12-parameter affine and 16 iteration nonlinear transformations) the images (for more details, see Ashburner and Friston [2005]). Because the purpose of this process is to produce custom symmetric tissue probability maps, Jacobian modulation was not applied [Good et al., 2001b]. The normalized and segmented images were averaged across the dataset to produce gray matter, white matter, and cerebrospinal fluid sample-specific templates. Each template was flipped and averaged with the unflipped template to create custom symmetrical gray matter, white matter, and cerebrospinal fluid templates [Dorsaint-Pierre et al., 2006; Eckert et al., 2008; Good et al., 2001a; Hervé et al., 2006; Huster et al., 2007; Kawasaki et al., 2008; Luders et al., 2004; Mühlau et al., 2007; Prinster et al., 2006; Shibata, 2007; Watkins et al., 2001]. Unified segmentation was then performed again using the custom symmetrical templates as priors. The normalized and segmented images were modulated to correct voxel signal intensity for volume displacement during normalization and reflect the volume of gray matter [Good et al., 2001b]. Gray matter asymmetry images were created of the original minus flipped images [Dorsaint-Pierre et al., 2006; Hervé et al., 2006; Shibata, 2007; Watkins et al., 2001]. A positive voxel value on the left side of the asymmetry image corresponded to a higher signal (i.e., more gray matter volume) on the left hemisphere than the right and vice versa. Because of the use of the symmetrical templates for spatial normalization, the asymmetry images were not in Montreal Neurological Institute (MNI) space. To spatially normalize to MNI space, the symmetrical gray matter template was registered

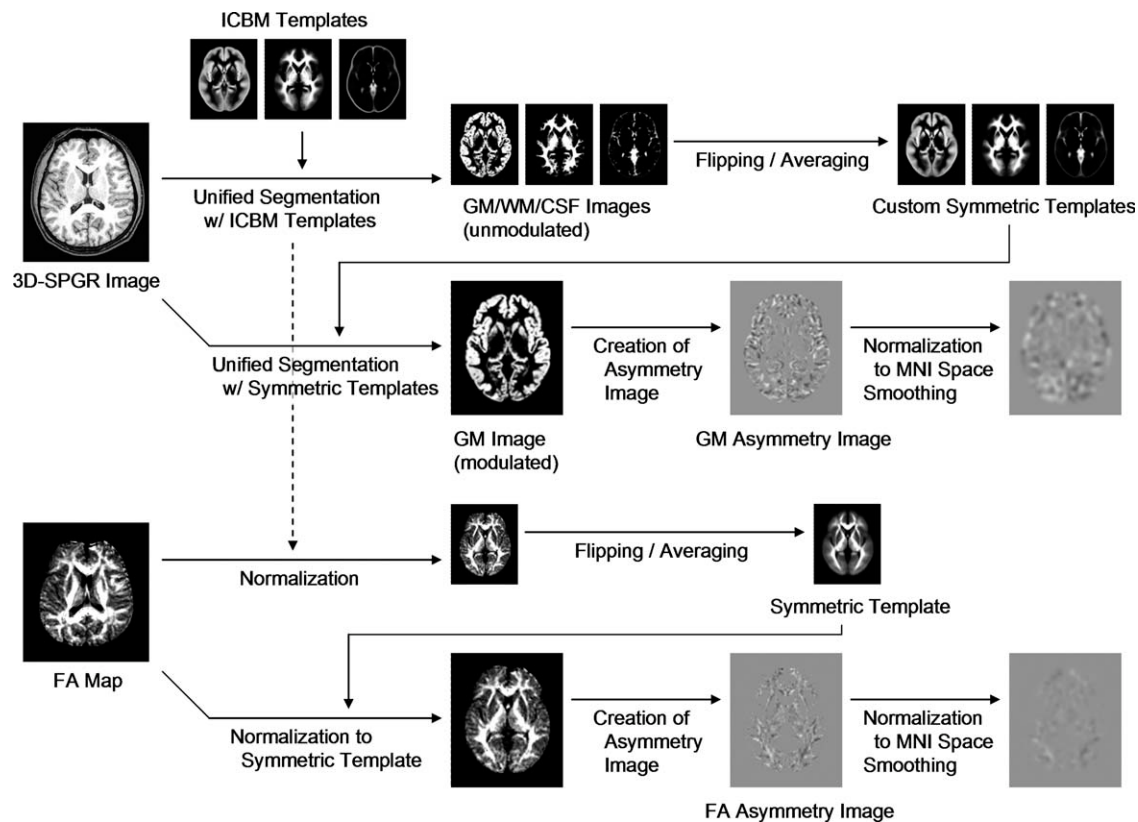


**Figure 1.**

Summary of image processing using statistical parametric mapping (SPM) 5 software. 3D-SPGR indicates three-dimensional spoiled-gradient recalled acquisition in the steady state; ICBM, The International Consortium for Brain Mapping; GM, gray matter; WM, white matter; CSF, cerebrospinal fluid; MNI, Montreal Neurological Institute; FA, fractional anisotropy.

(12-parameter affine and 16 iteration nonlinear transformations, whereby the nonlinear deformations were defined by a linear combination of three-dimensional discrete cosine transform basis functions [Ashburner and Friston, 1999]) to the nonsymmetrical gray matter template, and the derived transformation parameters were applied to the asymmetry images. The normalized asymmetry images were smoothed using an 8-mm kernel.

Modulated gray matter (or other tissue class) images are three-dimensional matrices where the intensity of each voxel is proportional to its volume within each voxel. With the use of the modulated images, gray and white matter volumes were calculated by multiplying the voxel intensity by the voxel volume and summing the results for all of the voxels. Global gray and white matter volumes were not normalized for head size.

### DTI Asymmetry Processing

The T2-weighted echo-planar images ( $b = 0 \text{ s/mm}^2$ ) were coregistered with the 3D-SPGR images, and the core-

gistration parameters were applied to the corresponding FA maps. The transformation parameters derived from the spatial normalization of the 3D-SPGR images onto the ICBM templates were also applied to the coregistered FA maps. The normalized FA maps were averaged across the dataset to produce a custom FA template. The template was flipped and averaged with the unflipped template to create a custom symmetrical FA template, which was smoothed using an 8-mm kernel. All the FA maps in native space were then registered (12-parameter affine and 16 iteration nonlinear transformations [Ashburner and Friston, 1999]) to the symmetrical FA template. FA asymmetry images were created of the original minus flipped images, which were thresholded at a FA value of 0.2 to minimize contributions from gray matter or cerebrospinal fluid. The asymmetry images were spatially normalized to MNI space using the transformation parameters derived from registering (12-parameter affine and 16 iteration nonlinear transformations [Ashburner and Friston, 1999]) the symmetrical FA template to the nonsymmetrical FA template. The normalized asymmetry images were smoothed using a 6-mm kernel.



## Statistical Analyses

Data were analyzed with SPM5 using the framework of the general linear model [Friston et al., 1995]. First, we identified areas of significant gray matter asymmetry using a one-sample *t* test with sex and age as covariates of no interest. Gray matter volume was normalized using whole brain volume. We also assessed the effect of sex on gray matter asymmetry using a two-sample *t* test with age as a covariate of no interest. Next, we identified areas of significant FA asymmetry using a one-sample *t* test with sex and age as covariates of no interest. No global normalization was applied. We also assessed the effect of sex on FA asymmetry using a two-sample *t* test with age as a covariate of no interest.

The left and right sides of asymmetry images are mirror images of each other. When dealing with asymmetry images, a single contrast gathers, on the left side of the images, the positive differences between the left and right hemisphere (leftward asymmetry), and, on the right side of the images, the positive differences between the right and left hemisphere (rightward asymmetry). Although this is convenient, this also results in doubling the number of tests inside a same contrast and thus overcorrection for multiple comparisons [Hervé et al., 2006]. Therefore, we computed two contrasts (left minus right and right minus left) on the sole left side of the asymmetry images. Only voxels with a probability greater than 0.1 and with a FA value greater than 0.2 were included for gray matter and FA asymmetry analyses, respectively. Significance levels for one-tailed *t* tests were set at  $P < 0.025$ , corrected for multiple comparisons using the family-wise error rate (voxel-level). The voxel size was 2 mm × 2 mm × 2 mm. Only clusters of at least 200 voxels are reported for both gray matter and FA asymmetry analyses.

## RESULTS

### Global Volumes

There was no correlation between age and gray matter volume ( $R^2 = 0.0020$ ,  $P = 0.65$ ) or white matter volume ( $R^2 = 0.032$ ,  $P = 0.061$ ) within the age range studied (21–29 years) (see Fig. 2). The mean gray and white matter volumes were significantly greater in males (gray matter,  $745.5 \pm 47.6$  mL; white matter,  $530.6 \pm 49.9$  mL) than in females (gray matter,  $670.8 \pm 44.4$  mL; white matter,  $461.9 \pm 36.9$  mL) ( $P < 0.0001$ , respectively).

### Gray Matter (Volume) Asymmetry

The voxel-based analysis of gray matter differences between the left and right hemispheres confirmed the well-known right frontal and left occipital petalias and leftward asymmetry of the planum temporale and transverse temporal (Heschl's) gyri (Fig. 3, Table I). There was a rightward asymmetry of the temporal pole. Leftward asymmetry was

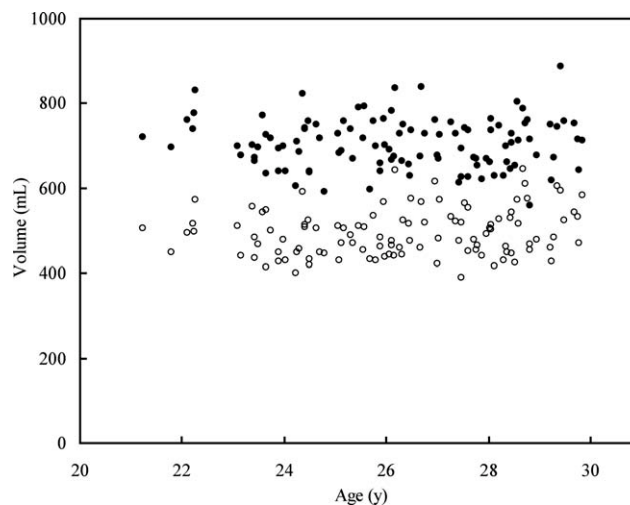


**Figure 2.**

Scatter plot of gray (black dots) and white matter (white dots) volume versus age.

also seen in anterior and superior portions of the insula, in the medial frontal gyrus, in the posterior parahippocampal gyrus, in the caudate head, and in the lateral cerebellum. Rightward asymmetry was seen in the inferior portion of the insula, in the medial occipital and parietal lobes, in the cingulate gyrus, and in the medial cerebellum. There was no significant difference in gray matter asymmetry between females and males (no cluster of  $\geq 10$  voxels).

### White Matter (FA) Asymmetry

The voxel-based analysis of white matter FA differences between the left and right hemispheres showed a leftward asymmetry of the posterior limb of the internal capsule, which extended inferiorly to the cerebral peduncle and superiorly to the superior corona radiata (Fig. 4, Table II). Leftward asymmetry was also seen in the arcuate fasciculus, in the cingulum, and in the cerebellum. Rightward asymmetry was seen in the frontal white matter, in the subinsular white matter (uncinate fasciculus), in the posterior corona radiata, and in the posterior corpus callosum. There was no significant difference in FA asymmetry between females and males (no cluster of  $\geq 10$  voxels).

### Post Hoc Analysis of the Relationship Between the Gray Matter Volume of the Planum Temporale and FA of the Arcuate Fasciculus

Leftward volume asymmetry of the planum temporale and leftward fractional anisotropy (FA) asymmetry of the arcuate fasciculus were simultaneously seen (see Fig. 5). Therefore, we evaluated the relationship between the gray matter volume of the planum temporale and FA of the arcuate fasciculus. A scatter plot of the relationship between

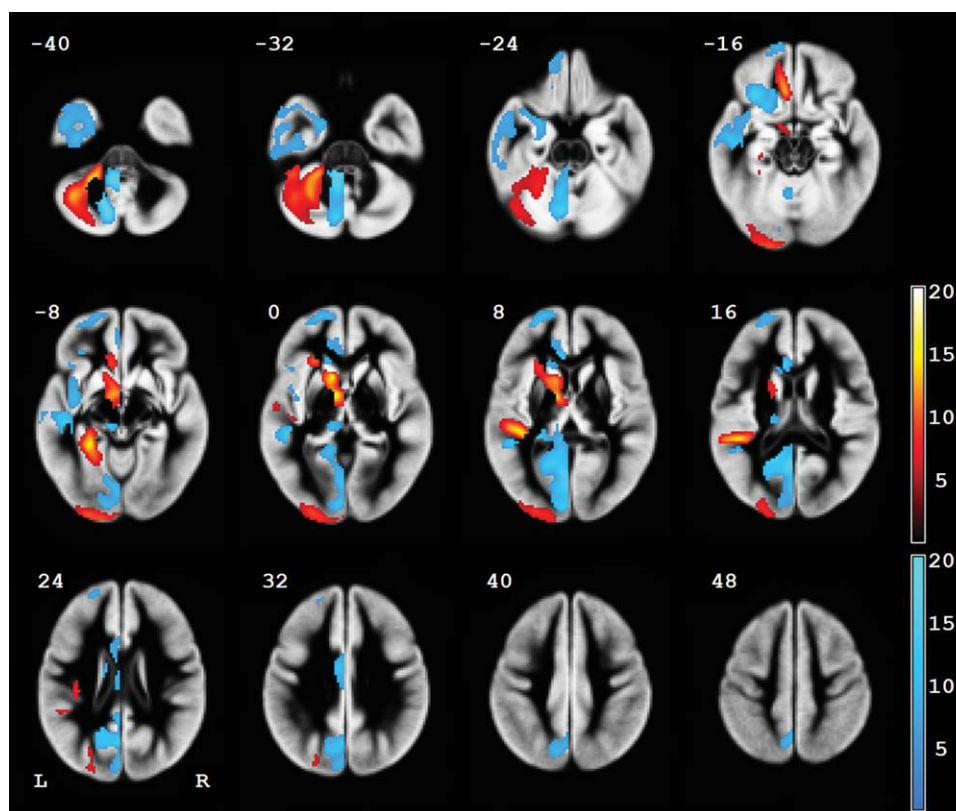


**Figure 3.**

Gray matter (volume) asymmetries in 109 right-handed healthy individuals aged 21–29 years. The color bars represent the *t* score at each voxel (red, leftward asymmetry; blue, rightward asymmetry). The voxel size is 2 mm × 2 mm × 2 mm. Only clusters of at least 200 voxels are shown.

the voxel values extracted from gray matter images at the statistical peak corresponding to the coordinates of the planum temporale ( $x = -38$ ,  $y = -34$ ,  $z = 10$ ) and the voxel values extracted from FA images at the statistical peak corresponding to the coordinates of the arcuate fasciculus ( $x = -42$ ,  $y = -42$ ,  $z = 8$ ) is presented in Figure 6. The voxel values extracted from gray matter images were normalized using whole brain volume. The gray matter volume of the planum temporale and FA of the arcuate fasciculus were positively related (Pearson correlation coefficient, 0.43;  $P < 0.0001$ ; major axis regression slope, 0.76; intercept, 0.19). When analyzed within each side, the relationship was significant on the left side (Pearson correlation coefficient, 0.20;  $P = 0.041$ ; major axis regression slope, 0.64; intercept, 0.23) but not on the right side (Pearson correlation coefficient, 0.13;  $P = 0.17$ ; major axis regression slope, 0.88; intercept, 0.15).

## DISCUSSION

The present study demonstrated a number of gray matter volume asymmetries (including the right frontal and left occipital petalias and leftward asymmetry of the pla-

num temporale) and white matter FA asymmetries (including leftward asymmetry of the arcuate fasciculus, cingulum, and corticospinal tract). Leftward volume asymmetry of the planum temporale and leftward FA asymmetry of the arcuate fasciculus was simultaneously demonstrated, and the gray matter volume of the planum temporale and FA of the arcuate fasciculus was positively related. The results suggest that leftward volume asymmetry of the planum temporale and leftward FA asymmetry of the arcuate fasciculus may be related.

The right frontal and left occipital petalias [Chiu and Damasio, 1980; LeMay, 1977; Toga and Thompson, 2003] and leftward asymmetry of the planum temporale [Geschwind and Levitsky, 1968; Toga and Thompson, 2003] are the most consistent structural asymmetries. The planum temporale is a triangular region that occupies the superior temporal plane and part of the classical Wernicke's area. It has often been assumed that leftward structural asymmetry of the pars opercularis and pars triangularis, frequently referred to as Broca's area, and exist in the human brain. However, postmortem and MR imaging studies have failed to consistently identify such a volumetric asymmetry [Keller et al., 2009]. In addition to replicating the presence of the

**TABLE I. Gray matter (volume) asymmetries**

Cluster size <sup>a</sup>	MNI coordinates			Peak <i>T</i>	<i>Z</i>	Region label <sup>b</sup>
	<i>x</i>	<i>y</i>	<i>z</i>			
Leftward asymmetries ( <i>L</i> > <i>R</i> )						
1,166	-8	-2	4	16.78	Inf	Caudate head
	-10	12	2	14.95	Inf	Caudate head
	-24	26	2	10.48	Inf	Insula
5,389	-22	-42	44	16.16	Inf	Cerebellum
	-26	-42	-8	14.58	Inf	Parahippocampal gyrus
	-38	-58	-38	14.43	Inf	Cerebellum
757	-38	-34	10	14.48	Inf	Superior temporal gyrus
	-46	-36	16	13.67	Inf	Superior temporal gyrus
	-34	-24	24	8.29	7.26	Insula
351	-6	26	-14	12.29	Inf	Medial frontal gyrus
344	-20	-44	66	8.77	7.58	Superior parietal lobule
	-18	-36	66	8.56	7.45	Postcentral gyrus
	-36	-46	58	7.51	6.71	Superior parietal lobule
Rightward asymmetries ( <i>L</i> < <i>R</i> )						
2,391	-14	-60	-44	27.49	Inf	Cerebellum
	-6	-42	-36	23.20	Inf	Cerebellum
	-8	-72	-38	20.67	Inf	Cerebellum
3,983	-6	-62	14	16.58	Inf	Posterior cingulate gyrus
	-18	-56	12	15.43	Inf	Posterior cingulate gyrus
	-2	-74	8	15.20	Inf	Cuneus
551	-32	26	-14	15.89	Inf	Inferior frontal gyrus
	-18	24	-16	10.00	Inf	Inferior frontal gyrus
3,298	-46	-28	-4	15.71	Inf	Superior temporal gyrus
	-46	-38	4	13.90	Inf	Superior temporal gyrus
	-50	-14	-16	11.74	Inf	Middle temporal gyrus
780	-8	26	12	13.46	Inf	Anterior cingulate gyrus
	-6	-6	32	10.90	Inf	Cingulate gyrus
	-2	42	-12	7.83	6.94	Medial frontal gyrus
979	-22	62	4	11.71	Inf	Superior frontal gyrus
	-22	58	18	9.11	7.80	Superior frontal gyrus
	-12	60	-20	8.93	7.69	Superior frontal gyrus

Note: MNI indicates Montreal Neurological Institute; inf, infinity.

<sup>a</sup>The voxel size is 2 mm × 2 mm × 2 mm. Only clusters of at least 200 voxels are reported.

<sup>b</sup>All regions reported in table are significant after family-wise error correction for multiple comparisons (resel count = 1016). Anatomical localization was determined with reference to the Talairach Daemon.

above well-established asymmetries (right frontal and left occipital petalias and leftward asymmetry of the planum temporale), our study revealed several other significant gray matter asymmetries, which are less established in the literature.

Some studies have explored cerebral asymmetry in normal individuals using VBM [Good et al., 2001a; Hervé et al., 2006; Watkins et al., 2001]. There are several inconsistencies in these studies. The reasons for this are likely due to heterogeneity of the populations from which study samples are drawn and differences in methods of analysis of the MR images. Good et al. [2001a] compared gray matter “volume” between the left and right hemispheres in 465 normal adults aged 17–79 years (398 right-handed and 67 left-handed). Watkins et al. [2001] compared gray matter “density” between the left and right hemispheres in 142 normal subjects aged 18–44 years (128 right-handed

and 14 left-handed). Hervé et al. [2006] examined gray matter volume asymmetry in 56 right-handed males (aged 18–34 years) and compared these subjects with 56 left-handed males. In this study, we investigated gray matter “volume” asymmetry in 109 right-handed healthy individuals aged 21–29 years. Previous studies were composed mainly of data from Caucasian samples, whereas our subjects were all Japanese. The right frontal and left occipital petalias (including rightward asymmetry of the temporal lobe) and leftward asymmetry of the planum temporale were consistently observed in these VBM studies (including our study). Leftward asymmetry of anterior and superior portions of the insula and rightward asymmetry of the anterior cingulate gyrus and medial occipital lobe were also consistently seen. We did not detect leftward asymmetry of Broca’s area as other VBM studies did not. Other asymmetries that we detected were not consistently

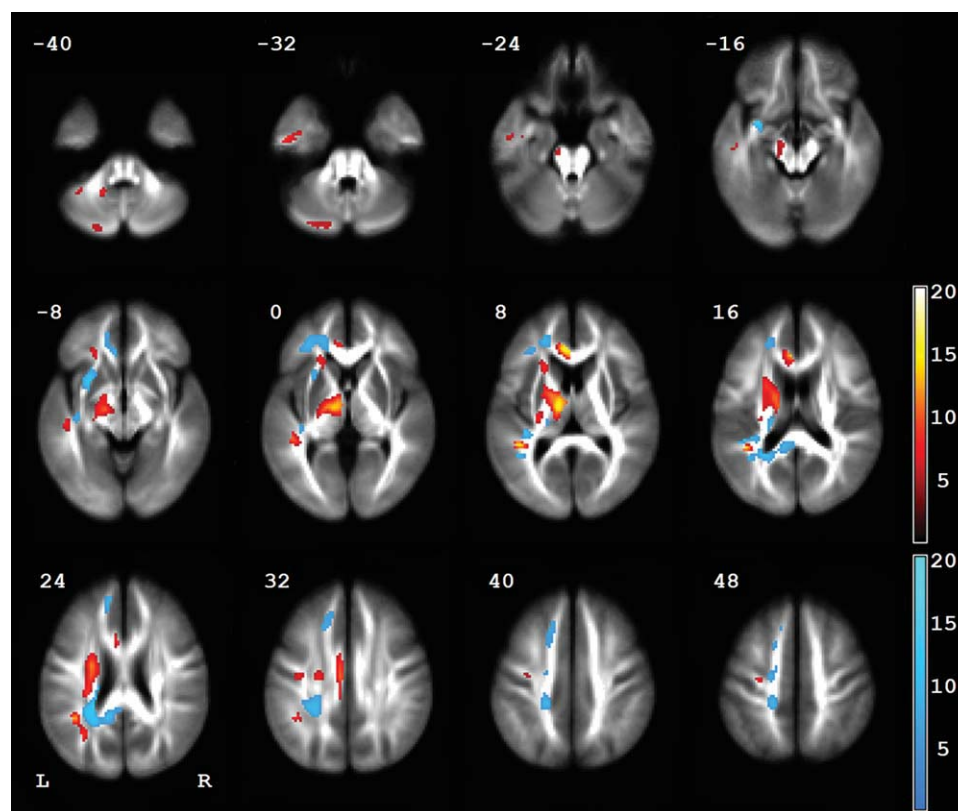


**Figure 4.**

White matter (fractional anisotropy) asymmetries in 109 right-handed healthy individuals aged 21–29 years. The color bars represent the *t* score at each voxel (red, leftward asymmetry; blue, rightward asymmetry). The voxel size is 2 mm × 2 mm × 2 mm. Only clusters of at least 200 voxels are shown.

observed in other studies. We did not detect any significant sex difference in gray matter asymmetry as other VBM studies did not (except for at the medial end of Heschl's sulcus, at the junction with the planum temporale, in Good et al.'s study [2001a]).

DTI is sensitive to subtle white matter changes. Previous ROI DTI studies have explored FA asymmetry in the arcuate fasciculus [Rodrigo et al., 2007], cingulum [Gong et al., 2005; Kubicki et al., 2003; Wang et al., 2004], uncinate fasciculus [Kubicki et al., 2002], subinsular white matter [Cao et al., 2003; Rodrigo et al., 2007], and corticospinal tract at the level of the internal capsule [Westerhausen et al., 2007]. The above regions of interest all showed a pattern of left-greater-than-right FA. The ROI-based approach requires a priori hypothesis to predefine the expected ROI.

A few studies have explored white matter asymmetry using a voxel-based analysis of diffusion tensor images [Ardekani et al., 2007; Büchel et al., 2004; Park et al., 2004]. Büchel et al. [2004] investigated FA asymmetry in 28 healthy individuals aged 21–40 years (19 right-handed and 9 left-handed). They detected a leftward asymmetry of the arcuate fasciculus. Park et al. [2004] explored FA asymme-

try in 32 right-handed healthy males (aged 30–55 years) and 23 male patients with schizophrenia. In healthy subjects, leftward asymmetry was found in the anterior part of the corpus callosum, in the cingulum, in the optic radiation, and in the superior cerebellar peduncle, whereas rightward asymmetry was found in the anterior limb of the internal capsule and the anterior limb's prefrontal regions, in the uncinate fasciculus, and in the superior and inferior aspect of the arcuate fasciculus. Ardekani et al. [2007] investigated FA asymmetry in 20 right-handed healthy individuals aged 26–69 years. In the young-age group, leftward asymmetry was found in the anterior limb of the external capsule, in the posterior limb of the internal capsule, in the thalamus, in the cerebral peduncle, and in the temporal-parietal regions. Rightward asymmetry was found in the genu, splenium, and body of the corpus callosum. There are several discrepancies in these studies, which may arise due to heterogeneity of the populations (e.g., sample size and age distribution) and differences in methods of analysis of the MR images. Previous studies were composed mainly of data from Caucasian samples, whereas our subjects were all Japanese. In our study, we



**TABLE II. White matter (fractional anisotropy) asymmetries**

Cluster size <sup>a</sup>	MNI coordinates			Peak <i>T</i>	<i>Z</i>	Region label <sup>b</sup>
	<i>x</i>	<i>y</i>	<i>z</i>			
Leftward asymmetries ( <i>L</i> > <i>R</i> )						
451	-6	36	8	15.86	Inf	Anterior cingulum
	-6	-12	32	10.29	Inf	Cingulum
	-6	18	22	7.49	6.69	Anterior cingulum
1,834	-14	-10	12	15.21	Inf	Thalamus
	-18	-2	12	13.02	Inf	Posterior limb of internal capsule
	-26	-2	22	11.02	Inf	Superior corona radiata
515	-42	-42	8	15.18	Inf	Arcuate fasciculus
	-40	-46	20	12.99	Inf	Arcuate fasciculus
	-42	-44	30	10.56	Inf	Arcuate fasciculus
659	-34	-58	-52	12.37	Inf	Cerebellum
	-28	-64	-54	10.12	Inf	Cerebellum
	-30	-74	-52	9.44	Inf	Cerebellum
Rightward asymmetries ( <i>L</i> < <i>R</i> )						
213	-30	2	-16	14.13	Inf	Uncinate fasciculus
1,311	-24	-36	26	13.13	Inf	Posterior corona radiata
	-44	-38	14	12.75	Inf	Temporal white matter
	-10	-44	20	12.73	Inf	Posterior corpus callosum
523	-22	42	4	9.55	Inf	Frontal white matter
	-32	36	2	9.52	Inf	Frontal white matter
	-4	32	-6	8.77	7.58	Anterior cingulum
297	-12	48	24	8.89	7.66	Frontal white matter
	-18	28	34	8.53	7.42	Frontal white matter
	-14	38	30	7.10	6.41	Frontal white matter

Note: MNI indicates Montreal Neurological Institute; Inf, infinity.

<sup>a</sup>The voxel size is 2 mm × 2 mm × 2 mm. Only clusters of at least 200 voxels are reported.

<sup>b</sup>All regions reported in table are significant after family-wise error correction for multiple comparisons (resel count = 272). Anatomical localization was determined with reference to the Talairach Daemon.

found a number of FA asymmetries including leftward asymmetry of the arcuate fasciculus, cingulum, and corticospinal tract, which was reported by previous ROI studies [Gong et al., 2005; Kubicki et al., 2003; Rodrigo et al., 2007; Wang et al., 2004; Westerhausen et al., 2007]. We did not find leftward asymmetry of the subinsular white matter (uncinate fasciculus), contrary to previous ROI studies

[Cao et al., 2003; Rodrigo et al., 2007]. This discrepancy may be due to the narrow structure of the subinsular region and differences in methods of analysis of the MR images. In addition to the above asymmetries, we detected leftward asymmetry of the cerebellum, and rightward asymmetry of the frontal white matter, posterior corona radiata, and posterior corpus callosum. We did not find

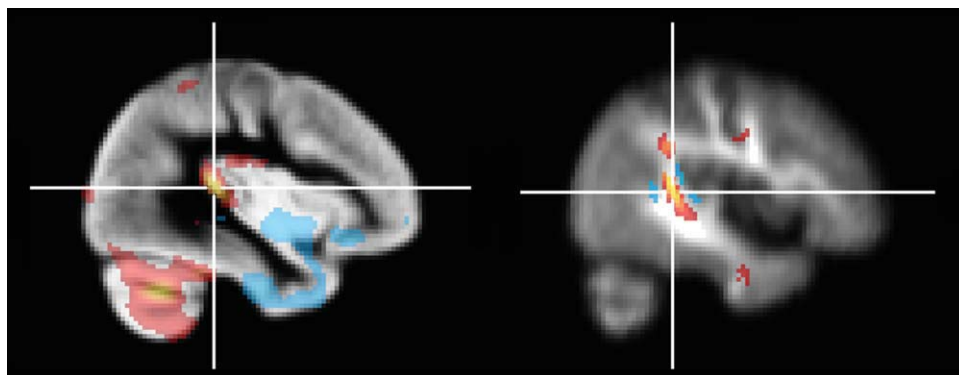


**Figure 5.**

Leftward volume asymmetry of the planum temporale ( $x = -38, y = -34, z = 10$ ) and leftward fractional anisotropy asymmetry of the arcuate fasciculus ( $x = -42, y = -42, z = 8$ ).

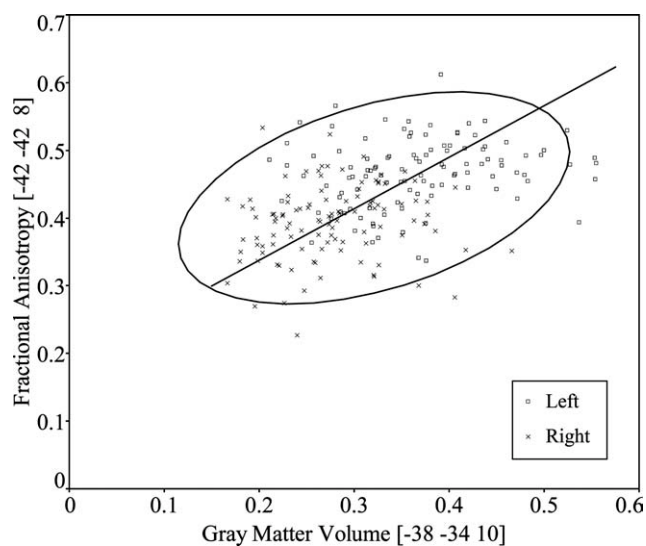


**Figure 6.**

Relationship between the gray matter volume of the planum temporale and fractional anisotropy of the arcuate fasciculus. The voxel values extracted from gray matter images at the statistical peak corresponding to the coordinates of the planum temporale ( $x = -38, y = -34, z = 10$ ) and the voxel values extracted from fractional anisotropy images at the statistical peak corresponding to the coordinates of the arcuate fasciculus ( $x = -42, y = -42, z = 8$ ) were positively related (Pearson correlation coefficient, 0.43;  $P < 0.0001$ ). The solid line indicates the major axis regression (slope, 0.76; intercept, 0.19). The ellipse indicates the 95% bivariate normal ellipse. The voxel values extracted from gray matter images were normalized using whole brain volume.

any significant difference in FA asymmetry between females and males. In Westerhausen et al.'s study [2007], where they examined FA asymmetry in the corticospinal tract at the level of the internal capsule, there was no significant interaction of sex and laterality. Other studies did not assess the effect of sex on FA asymmetry. These studies included a relatively small number of subjects with a wide age range. To our knowledge, our study is the first study that examined the effect of sex on FA asymmetry using a whole-brain approach. Our study showed no significant effect of sex on FA asymmetry. Our study included a large number of subjects aged 21–29 years.

The arcuate fasciculus is the tract that connects the frontal and parietotemporal language areas (Broca's and Wernicke's area). Some studies have showed the potential relationship between asymmetry of the arcuate fascicle and functional lateralization of language [Barrick et al., 2007; Powell et al., 2006]. Our study simultaneously demonstrated leftward volume asymmetry of the planum temporale and leftward FA asymmetry of the arcuate fasciculus. The gray matter volume of the planum temporale and FA of the arcuate fasciculus was positively related. The results suggest that leftward volume asymmetry of

the planum temporale and leftward FA asymmetry of the arcuate fasciculus may be related.

FA is the most widely used diffusion parameter in clinical studies [Smith et al., 2006]. A related scalar measure, geodesic anisotropy (GA), has recently been developed as an alternative to FA [Batchelor et al., 2005]. GA measures the distance of a diffusion tensor to the nearest isotropic tensor, computed intrinsically on the manifold of positive-definite symmetric diffusion tensors. Jahanshad et al. [2009] have investigated genetic influences on asymmetry of FA and GA. Fiber asymmetry was most strongly genetically influenced in frontal and occipital lobes. Statistical frameworks for tensor analysis have recently developed [Arsigny et al., 2006; Lee et al., 2007, 2009; Verma et al., 2006; Whitcher et al., 2007], although it is not yet a common practice to use them for statistical inferences in DTI [Pasternak et al., 2010]. Statistical hypothesis testing on the diffusion tensor, instead of scalar summaries derived from it, could provide greater statistical power, because there are more measurements available in the full tensor. By reducing the full diffusion tensor to scalar measures of diffusion anisotropy, potentially relevant information may be missed. However, scalar measures are somewhat more readily interpretable than the diffusion tensor itself.

There were several limitations to this study. First, we restricted the study to right-handed subjects. Therefore, we could not evaluate the effect of handedness on cerebral asymmetry. Although the results are not directly applicable to left-handers, however, there is strength in not being confounded by potential handedness-related differences. Second, in the period when this study started, it was difficult to acquire diffusion tensor images with isotropic spatial resolution and a large number of gradient sampling orientations on the version of MR system used. Low spatial and angular resolutions were also limitations. Further evaluation using updated imaging sequences and parameters would be required to replicate the results in this study. Third, we normalized gray matter images or FA maps using custom symmetric templates and then normalized the asymmetry images created from them to MNI space. These steps may potentially cause blurring in the final images; however, the number of normalization steps is the same as the standard VBM method using DARTEL [Ashburner, 2007]. Fourth, in this study, we used a VBM method, which is the most commonly used tool to identify differences in the local composition of brain tissue. Tensor-based morphometry (TBM) is one image analysis technique that identifies regional structural differences from the gradients of the nonlinear deformation fields that align images to a common anatomical template. At each voxel, a Jacobian determinant value indicates local volume excess or deficit relative to the corresponding anatomical structures in the template. TBM has potential advantages over VBM; however, it requires computationally expensive estimation of high-resolution deformation fields that map each individual brain to a standard reference. Finally, we used a voxel-based analysis to evaluate white matter FA

asymmetry in this study. VBM analyses of diffusion tensor data have some problems [Jones et al., 2005; Smith et al., 2006], although many studies have successfully detected age- or disease-related changes with use of VBM analyses of diffusion tensor data. Further evaluation using updated imaging sequences and more sophisticated analysis methods would be necessary to replicate the results of our study.

## CONCLUSION

We investigated cerebral asymmetry using VBM and DTI in 109 right-handed healthy individuals aged 21–29 years. We found a number of gray matter volume asymmetries (including the right frontal and left occipital petalias and leftward asymmetry of the planum temporale) and white matter FA asymmetries (including leftward asymmetry of the arcuate fasciculus, cingulum, and corticospinal tract). There was no significant effect of sex on gray and white matter asymmetry. Leftward volume asymmetry of the planum temporale and leftward FA asymmetry of the arcuate fasciculus were simultaneously demonstrated. The gray matter volume of the planum temporale and FA of the arcuate fasciculus was positively related. Our results are free from the potential confounding effects of aging and handedness and suggest that leftward volume asymmetry of the planum temporale and leftward FA asymmetry of the arcuate fasciculus may be related.

## REFERENCES

- Abe O, Yamasue H, Aoki S, Suga M, Yamada H, Kasai K, Masutani Y, Kato N, Kato N, Ohtomo K (2008): Aging in the CNS: Comparison of gray/white matter volume and diffusion tensor data. *Neurobiol Aging* 29:102–116.
- Ardekani S, Kumar A, Bartzokis G, Sinha U (2007): Exploratory voxel-based analysis of diffusion indices and hemispheric asymmetry in normal aging. *Magn Reson Imaging* 25:154–167.
- Arsigny V, Fillard P, Pennec X, Ayache N (2006): Log-Euclidean metrics for fast and simple calculus on diffusion tensors. *Magn Reson Med* 56:411–421.
- Ashburner J (2007): A fast diffeomorphic image registration algorithm. *NeuroImage* 38:95–113.
- Ashburner J, Friston KJ (1999): Nonlinear spatial normalization using basis functions. *Hum Brain Mapp* 7:254–266.
- Ashburner J, Friston KJ (2000): Voxel-based morphometry—The methods. *NeuroImage* 11:805–821.
- Ashburner J, Friston KJ (2005): Unified segmentation. *NeuroImage* 26:839–851.
- Barrick TR, Lawes IN, Mackay CE, Clark CA (2007): White matter pathway asymmetry underlies functional lateralization. *Cereb Cortex* 17:591–598.
- Basser PJ, Mattiello J, LeBihan D (1994): MR diffusion tensor spectroscopy and imaging. *Biophys J* 66:259–267.
- Batchelor PG, Moakher M, Atkinson D, Calamante F, Connelly A (2005): A rigorous framework for diffusion tensor calculus. *Magn Reson Med* 53:221–225.
- Büchel C, Raedler T, Sommer M, Sach M, Weiller C, Koch MA (2004): White matter asymmetry in the human brain: A diffusion tensor MRI study. *Cereb Cortex* 14:945–951.
- Càmara E, Bodammer N, Rodríguez-Fornells A, Tempelmann C (2007): Age-related water diffusion changes in human brain: A voxel-based approach. *NeuroImage* 34:1588–1599.
- Cao Y, Whalen S, Huang J, Berger KL, DeLano MC (2003): Asymmetry of subinsular anisotropy by in vivo diffusion tensor imaging. *Hum Brain Mapp* 20:82–90.
- Chiu HC, Damasio AR (1980): Human cerebral asymmetries evaluated by computed tomography. *J Neurol Neurosurg Psychiatry* 43:873–878.
- Dorsaint-Pierre R, Penhune VB, Watkins KE, Neelin P, Lerch JP, Bouffard M, Zatorre RJ (2006): Asymmetries of the planum temporale and Heschl's gyrus: Relationship to language lateralization. *Brain* 129:1164–1176.
- Eckert MA, Lombardino LJ, Walczak AR, Bonihla L, Leonard CM, Binder JR (2008): Manual and automated measures of superior temporal gyrus asymmetry: Concordant structural predictors of verbal ability in children. *NeuroImage* 41:813–822.
- First MB, Spitzer RL, Gibbon M, Williams JB (1997): Structured clinical interview for DSM-IV axis I disorders: Non-patient edition. Biometrics Research Department, NewYork State Psychiatric Institute, New York.
- Friston KJ, Holmes AP, Worsley KJ, Poline JP, Frith CD, Frackowiak RS (1995): Statistical parametric maps in functional imaging: A general linear approach. *Hum Brain Mapp* 2:189–210.
- Geschwind N, Levitsky W (1968): Human brain: Left-right asymmetries in temporal speech region. *Science* 161:186–187.
- Gong G, Jiang T, Zhu C, Zang Y, Wang F, Xie S, Xiao J, Guo X (2005): Asymmetry analysis of cingulum based on scale-invariant parameterization by diffusion tensor imaging. *Hum Brain Mapp* 24:92–98.
- Good CD, Johnsrude I, Ashburner J, Henson RN, Friston KJ, Frackowiak RS (2001a): Cerebral asymmetry and the effects of sex and handedness on brain structure: A voxel-based morphometric analysis of 465 normal adult human brains. *NeuroImage* 14:685–700.
- Good CD, Johnsrude IS, Ashburner J, Henson RN, Friston KJ, Frackowiak RS (2001b): A voxel-based morphometric study of ageing in 465 normal adult human brains. *NeuroImage* 14:21–36.
- Griffiths TD, Warren JD (2002): The planum temporale as a computational hub. *Trends Neurosci* 25:348–353.
- Haselgrove JC, Moore JR (1996): Correction for distortion of echo-planar images used to calculate the apparent diffusion coefficient. *Magn Reson Med* 36:960–964.
- Hervé PY, Crivello F, Percey G, Mazoyer B, Tzourio-Mazoyer N (2006): Handedness and cerebral anatomical asymmetries in young adult males. *NeuroImage* 29:1066–1079.
- Hirayasu Y, McCarley RW, Salisbury DF, Tanaka S, Kwon JS, Frumin M, Snyderman D, Yurgelun-Todd D, Kikinis R, Jolesz FA, Shenton ME (2000): Planum temporale and Heschl gyrus volume reduction in schizophrenia: A magnetic resonance imaging study of first-episode patients. *Arch Gen Psychiatry* 57:692–699.
- Hsu JL, Leemans A, Bai CH, Lee CH, Tsai YF, Chiu HC, Chen WH (2008): Gender differences and age-related white matter changes of the human brain: A diffusion tensor imaging study. *NeuroImage* 39:566–577.
- Huster RJ, Westerhausen R, Kreuder F, Schweiger E, Wittling W (2007): Morphologic asymmetry of the human anterior cingulate cortex. *NeuroImage* 34:888–895.
- Jahanshad N, Lee AD, Lepore N, Brun C, Barysheva M, Chou Y, Toga AW, McMahon KL, de Zubicaray GI, Wright MJ, Thompson PM (2009): Genetics of white matter asymmetry mapped using diffusion tensor anisotropy measures in 100 twins.

- Proceedings of the 15th Annual Meeting of the Organization for Human Brain Mapping, San Francisco.
- Jones DK, Symms MR, Cercignani M, Howard RJ (2005): The effect of filter size on VBM analyses of DT-MRI data. *NeuroImage* 26:546–554.
- Kawasaki Y, Suzuki M, Takahashi T, Nohara S, McGuire PK, Seto H, Kurachi M (2008): Anomalous cerebral asymmetry in patients with schizophrenia demonstrated by voxel-based morphometry. *Biol Psychiatry* 63:793–800.
- Keller SS, Crow T, Foundas A, Amunts K, Roberts N (2009): Broca's area: Nomenclature, anatomy, typology and asymmetry. *Brain Lang* 109:29–48.
- Kubicki M, Westin CF, Maier SE, Frumin M, Nestor PG, Salisbury DF, Kikinis R, Jolesz FA, McCarley RW, Shenton ME (2002): Uncinate fasciculus findings in schizophrenia: A magnetic resonance diffusion tensor imaging study. *Am J Psychiatry* 159:813–820.
- Kubicki M, Westin CF, Nestor PG, Wible CG, Frumin M, Maier SE, Kikinis R, Jolesz FA, McCarley RW, Shenton ME (2003): Cingulate fasciculus integrity disruption in schizophrenia: A magnetic resonance diffusion tensor imaging study. *Biol Psychiatry* 54:1171–1180.
- Kwon JS, McCarley RW, Hirayasu Y, Anderson JE, Fischer IA, Kikinis R, Jolesz FA, Shenton ME (1999): Left planum temporale volume reduction in schizophrenia. *Arch Gen Psychiatry* 56:142–148.
- Lee AD, Leporé N, Leporé F, Alary F, Voss P, Chou Y, Brun C, Barysheva M, Toga AW, Thompson PM (2007): Brain differences visualized in the blind using tensor manifold statistics and diffusion tensor imaging. Proceedings of the 2007 International Conference Frontiers in the Convergence of Bioscience and Information Technologies, Jeju Island.
- Lee AD, Leporé N, Brun C, Chou Y, Barysheva M, Chiang M, Madsen SK, de Zubicaray GI, McMahon KL, Wright MJ, Toga AW, Thompson PM (2009): Tensor-based analysis of genetic influences on brain integrity using DTI in 100 twins. Proceedings of the 12th International Conference on Medical Image Computing and Computer Assisted Intervention, London.
- LeMay M (1977): Asymmetries of the skull and handedness. *Phrenology revisited*. *J Neurol Sci* 32:243–253.
- Luders E, Gaser C, Jancke L, Schlaug G (2004): A voxel-based approach to gray matter asymmetries. *NeuroImage* 22:656–664.
- Mangin JF, Poupon C, Clark C, Le Bihan D, Bloch I (2002): Distortion correction and robust tensor estimation for MR diffusion imaging. *Med Image Anal* 6:191–198.
- Moseley ME, Cohen Y, Kucharczyk J, Mintorovitch J, Asgari HS, Wendland MF, Tsuruda J, Norman D (1990): Diffusion-weighted MR imaging of anisotropic water diffusion in cat central nervous system. *Radiology* 176:439–445.
- Mühlau M, Gaser C, Wohlschläger AM, Weindl A, Städtler M, Valet M, Zimmer C, Kassubek J, Peinemann A (2007): Striatal gray matter loss in Huntington's disease is leftward biased. *Mov Disord* 22:1169–1173.
- Nucifora PG, Verma R, Melhem ER, Gur RE, Gur RC (2005): Leftward asymmetry in relative fiber density of the arcuate fasciculus. *Neuroreport* 16:791–794.
- Oldfield RC (1971): The assessment and analysis of handedness: The Edinburgh inventory. *Neuropsychologia* 9:97–113.
- Park HJ, Westin CF, Kubicki M, Maier SE, Niznikiewicz M, Baer A, Frumin M, Kikinis R, Jolesz FA, McCarley RW, Shenton ME (2004): White matter hemisphere asymmetries in healthy subjects and in schizophrenia: A diffusion tensor MRI study. *NeuroImage* 23:213–223.
- Pasternak O, Sochen N, Basser PJ (2010): The effect of metric selection on the analysis of diffusion tensor MRI data. *NeuroImage* 49:2190–2204.
- Powell HW, Parker GJ, Alexander DC, Symms MR, Boulby PA, Wheeler-Kingshott CA, Barker GJ, Noppeney U, Koeppe MJ, Duncan JS (2006): Hemispheric asymmetries in language-related pathways: A combined functional MRI and tractography study. *NeuroImage* 32:388–399.
- Prinster A, Quarantelli M, Orefice G, Lanzillo R, Brunetti A, Mollica C, Salvatore E, Morra VB, Coppola G, Vacca G, Alfano B, Salvatore M (2006): Grey matter loss in relapsing-remitting multiple sclerosis: A voxel-based morphometry study. *NeuroImage* 29:859–867.
- Rodrigo S, Naggara O, Oppenheim C, Golestani N, Poupon C, Cointepas Y, Mangin JF, Le Bihan D, Meder JF (2007): Human subinsular asymmetry studied by diffusion tensor imaging and fiber tracking. *Am J Neuroradiol* 28:1526–1531.
- Rovaris M, Bozzali M, Iannucci G, Ghezzi A, Caputo D, Montanari E, Bertolotto A, Bergamaschi R, Capra R, Mancardi GL, Martinelli V, Comi G, Filippi M (2002): Assessment of normal-appearing white and gray matter in patients with primary progressive multiple sclerosis: A diffusion-tensor magnetic resonance imaging study. *Arch Neurol* 59:1406–1412.
- Shibata DK (2007): Differences in brain structure in deaf persons on MR imaging studied with voxel-based morphometry. *Am J Neuroradiol* 28:243–249.
- Smith SM, Jenkinson M, Johansen-Berg H, Rueckert D, Nichols TE, Mackay CE, Watkins KE, Ciccarelli O, Cader MZ, Matthews PM, Behrens TE (2006): Tract-based spatial statistics: Voxelwise analysis of multi-subject diffusion data. *NeuroImage* 31:1487–1505.
- Takahashi T, Suzuki M, Zhou SY, Tanino R, Hagino H, Kawasaki Y, Matsui M, Seto H, Kurachi M (2006): Morphologic alterations of the parcellated superior temporal gyrus in schizophrenia spectrum. *Schizophr Res* 83:131–143.
- Taki Y, Goto R, Evans A, Zijdenbos A, Neelin P, Lerch J, Sato K, Ono S, Kinomura S, Nakagawa M, Sugiura M, Watanabe J, Kawashima R, Fukuda H (2004): Voxel-based morphometry of human brain with age and cerebrovascular risk factors. *Neurobiol Aging* 25:455–463.
- Toga AW, Thompson PM (2003): Mapping brain asymmetry. *Nat Rev Neurosci* 4:37–48.
- Verma R, Davatzikos C (2006): Manifold based analysis of diffusion tensor images using isomaps. Proceedings of the 3rd IEEE International Symposium on Biomedical Imaging, Arlington.
- Wang F, Sun Z, Cui L, Du X, Wang X, Zhang H, Cong Z, Hong N, Zhang D (2004): Anterior cingulum abnormalities in male patients with schizophrenia determined through diffusion tensor imaging. *Am J Psychiatry* 161:573–575.
- Watkins KE, Paus T, Lerch JP, Zijdenbos A, Collins DL, Neelin P, Taylor J, Worsley KJ, Evans AC (2001): Structural asymmetries in the human brain: A voxel-based statistical analysis of 142 MRI scans. *Cereb Cortex* 11:868–877.
- Werring DJ, Brassat D, Droogan AG, Clark CA, Symms MR, Barker GJ, MacManus DG, Thompson AJ, Miller DH (2000): The pathogenesis of lesions and normal-appearing white matter changes in multiple sclerosis: A serial diffusion MRI study. *Brain* 123:1667–1676.
- Westerhausen R, Huster RJ, Kreuder F, Wittling W, Schweiger E (2007): Corticospinal tract asymmetries at the level of the internal capsule: Is there an association with handedness? *NeuroImage* 37:379–386.
- Whitcher B, Wisco JJ, Hadjikhani N, Tuch DS (2007): Statistical group comparison of diffusion tensors via multivariate hypothesis testing. *Magn Reson Med* 57:1065–1074.